Int. J. Electrochem. Sci., 3 **(2008)** 1316 - 1324

International Journal of ELECTROCHEMICAL SCIENCE
www.electrochemsci.org

Effects of Ligands on Electroless Ni-Fe-P thin Films from Sulphate Bath

Wei-Qing Huang, Gui-Fang Huang[*]*, Ling-Ling Wang, Xiao-Gang Shi*

College of Physics and microelectronics Science, Hunan University, Changsha 410082, China
[*]E-mail: huanggfhao@yahoo.com

Received: 1 September 2008 / *Accepted:* 4 September 2008 / *Published:* 4 October 2008

Ni-Fe-P thin film was prepared by electroless deposition from sulphate bath. The effects of ligands, such as tri-sodium citrate(NaCit) and/or tri-ammonium citrate(NHCit), on the deposition process, deposition rate, composition, and structure of Ni-Fe-P thin film were investigated. It is found that adding NHCit to the electroless deposition systems made them more polarized, shifted the deposition potential to positive direction and decreased the deposition rate. When the total concentration of NaCit and NHCit is fixed in bath, the increasing of the ratio of [NHCit]/[NaCit+NHCit] in bath increases the amorphous degree of thin films corresponding to the increase of phosphorus content resulted from the competitive reduction of several ions. The work is helpful for the structure optimization and performance improvement of electroless thin films.

Keywords: thin films [A], X-ray diffraction [D], Electroless deposition[B]

1. INTRODUCTION

It is well known that electroless deposition process is an autocatalytic process with the metal as a final product due to the chemical reduction of the metal cations through reducing agents in the bath. In the electroless bath, metal salt and reducing agent are the essential ingredients. Another important component is ligand, which is usually added in the bath to form complexes with metal ions to insure the plating bath stability, reasonable metal deposition rate and acceptable quality of thin films by controlling the free metal ions available to the reaction, the reduction of metal ion, nucleation and development of the thin film. Many organic and inorganic compounds can be used as ligands in the electroless bath. In plating bath with ligands, almost all the metal ions exist in the form of complex, so it is the metal complexes instead of the free metal ions to be the precursors.

The effects of ligands on the electroless Ni-P alloy and copper deposition were investigated extensively [1-8]. Vaskelis et al. found that small addition of ammonia can accelerated the copper

electroless deposition by a factor of 2-4, while the effect of thio-compounds is not sufficient at low concentration[2, 7-8]. The deposition rate and composition of electroless Ni-P thin films was also found to be a function of concentration of ligands[5-6].

The Fe, Ni alloys are known for their excellent magnetic properties and applied widely in various fields. Compared with other methods to prepare Fe, Ni films, electroless deposition can be used to produce uniformly thick, hard and corrosion-resistant films on various material substrates with different shapes[9-16]. Electroless Ni–Fe–P film was first obtained by Wang et al[11]. Previous studies have reported the effect of pH and mole ratios of $FeSO_4$/($NiSO_4$+$FeSO_4$) in the bath on the deposition rate, composition, structure and microhardness of Ni-Fe-P electroless thin films[11,16]. However, the effects of ligands on the electroless Ni-Fe-P deposition are still open for investigation.

A detailed understanding of the species formed in solution is essential for the understanding of the factors controlling the performance of the elextroless bath. For example, NH_3 is a well known ligand, forming complexes of the type $[M(NH_3)_n]^{2+}$, where M could be Ni, Co, Fe and many other metals, and *n* could assume values between 2 and 6. All such complexes are good precursors for the deposition of the metal. Citrate is an excellent ligand that can stabilize the same metal ions in alkaline solutions, forming a complex such as [MCit]-. $[MCit_2]^{4-}$ and $[MHCit]^{2-}$, which, for example, binds M^{2+} so strongly that it can hardly be deposited. In this work, we investigate the effects of two ligands – tri-ammonium citrate and tri-sodium citrate on the electroless Ni-Fe-P thin films from alkaline solutions. XRD, SEM, gravimetric and electrochemical measurements were employed to characterize the Ni-Fe-P thin films.

2. EXPERIMENTAL PART

The copper was used as substrate, which was polished orderly with #600, #1200, and #2000 emery papers, and then rinsed by de-ionized water, diluted HCl, de-ionized water, acetone, de-ionized water, alcohol in sequence prior to deposition. A basic hypophosphite reduced electroless sulphate bath was chosen as the plating bath, where nickel sulphate and iron sulphate were used as the source of metals in the bath, and sodium hypophosphite served as the reductant and source of phosphorus. NaCit and NHCit acted as ligands and the total concentration of them was 0.165 M in the bath. Chemical compositions of electroless Ni-Fe- P plating bath are listed in table 1. The pH of the solution was adjusted to about 10 using $NH_3.H_2O$ and the bath temperature was 80 ± 1^oC. As copper is not a catalytic substrate for chemical deposition from hypophosphite solutions, the Ni-Fe-P deposition was initiated galvanically using aluminum at the beginning of the electroless process[17].

Table 1. Chemical compositions of electroless Ni-Fe-P plating bath

reagent	$(NH_4)_3C_6H_5O_7$	$(Na)_3C_6H_5O_7.2H_2O$	$FeSO_4.7H_2O$	$NiSO_4.6H_2O$	$NaH_2PO_2.H_2O$	$C_{12}H_{12}O_{11}$	$NH_3.H_2O$
Concentration, mM	0-165	0-165	54	29	311	6	25 mL/L

To perform the gravimetrical measurements, electroless Ni-Fe-P thin films were prepared on copper foils. The weight of thin films was calculated by weighing the samples before and after deposition by electronic microbalance model HT-300. The average deposition rate was determined by dividing the thin film mass by the surface area of substrate and deposition time.

Polarization experiments were carried out in a three-compartment cell with the electrochemical analyzer CHI-660B. A platinum foil with size 20mm × 40mm was used as an auxiliary electrode and a saturated calomel electrode were used as reference electrode. The working electrode was the copper electrode (ϕ = 19 mm) embedded in an epoxy resin. In order to simulate partial cathodic or anodic reactions, the investigation of the electrolytes in the absence of either the reductant $Na_2H_2PO_2$ (oxidation solution) or the metal salts $FeSO_4$ and $NiSO_4$ (reducing solution) was carried out. The polarization curves were obtained by scanning the potential in the range ±150 mV of the mixed potential E_{mix}, and the scanning rate was 1 mV s^{-1}.

The surface morphologies and compositions of the thin films were examined using scanning electron microscopy (SEM, JEOL JSM－6700) combined with energy dispersive spectrometry (EDS). The structure of the thin film was analyzed by XRD (Siemens D5000).

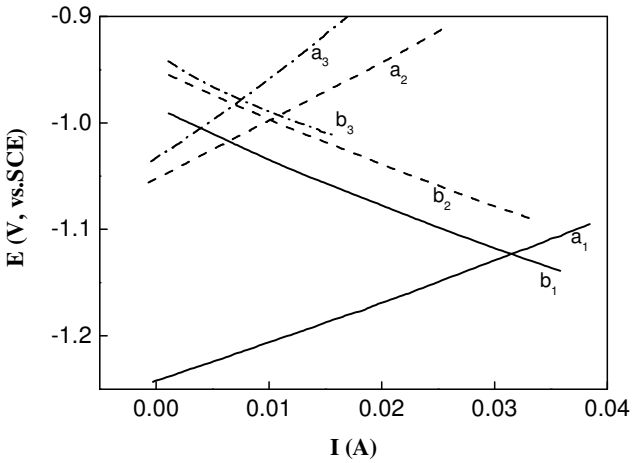

Figure 1. *I–E* curves for reduction of metal ions and for oxidation of hypophosphite. a_1, a_2, and a_3 are anodic oxidation curves, b_1, b_2, and b_3 are cathodic reduction curves. The subscripts 1, 2, and 3 denote the ratio of [NHCit]/[NaCit+NHCit] being 0, 0.5, and 1, respectively.

3. RESULTS AND DISCUSSION

3.1. Effects of ligands on the electroless Ni-Fe-P deposition process

In order to clarify the effects of ligands on Ni-Fe-P electroless deposition process, studies of independent partial reactions were performed firstly. The polarization measurements were carried out in the absence of either metal salts $FeSO_4$ and $NiSO_4$ (i.e., partial anodic curve) or reductant $H_2PO_2^-$ (i.e., partial cathodic curve). Fig.1 shows that the cathodic and anodic curves intersect at one point with

the ordinate and abscissa depending on the ligand species and concentration in the bath. In terms of the mixed potential theory, the coordinates of the intersection of these two polarization curves represent mixed potential (ordinate) and deposition current (abscissa), i.e., the mixed potential in volts *vs.* SCE electrode and the current in *A* are the function of the ligands.

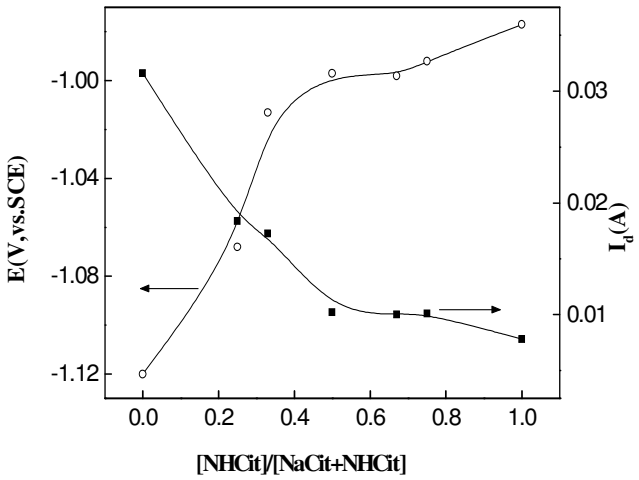

Figure 2. The dependences of the mixed potential and deposition current on the ratio of [NHCit]/[NaCit+NHCit]

Figure 2 presents the dependence of the mixed potential and deposition current on the ligands, as derived from experimental polarization measurements. It can be seen that mixed potential shifts positively, and deposition current(*i.e.*, deposition rate) decreases with the ratio of [NHCit]/[NaCit+NHCit] increasing.

The resistances for cathodic and anodic reactions (*R*pc and *R*pa) derived from the polarization curves are listed in Table 2. From the Table 2, one can see that the *R*pa and *R*pc increase with the increase of [NHCit]/[NaCit+NHCit]. This indicates that the addition of NHCit increases the anodic reaction resistance, thus inhibits the oxidation of $H_2PO_2^-$ and the formation of Ni-Fe-P thin films.

Table 2. The resistances for cathodic and anodic reaction (*R*pc and *R*pa) derived from the polarization curves

[NHCit]/[NaCit+NHCit]	0	0.5	1
*R*pc	4.26	4.34	5.23
*R*pa	3.83	5.49	7.83

With the addition of NaCit and/or NHCit in the electroless bath, almost all the metal ions exist in the form of complex. According to the stepwise deprotonation of citric and the speciation of

ammonia with increasing pH, the main citrate species is Cit^{3-} and $HCit^{4-}$, while the main species of ammonia is NH_3 in the pH value of 10[18]. Beside the formation of $[NiCit]^-$, $[FeCit]^-$, $[NiHCit]^{2-}$, and $[FeHCit]^{2-}$, $[Ni(NH_3)_n]^{2+}$ and $[Fe(NH_3)_n]^{2+}$ also formed with the addition of NHCit. The formation of complexes $[Ni(NH_3)_n]^{2+}$ and $[Fe(NH_3)_n]^{2+}$, which act as precursors for the deposition of the metal, increases the cathodic polarization and decreases the deposition rate.

3.2. Dependence of the deposition rate on ligands

As discussed in the previous section, the abscissa of intersection represents the deposition current in *A*. The instantaneous deposition rate, v_2(mg/cm^2·h), can be calculated from the deposition current, i_{dep}, using Faraday's law

$$v_2 = \frac{i_{dep}}{F}\frac{W}{n} = 0.373Ni_{dep} = 10.82i_{dep}(mg \cdot cm^{-2} \cdot h^{-1}) \qquad (1)$$

where F is the Faraday constant, W the average atomic weight of thin film (supposing W= 58), n the number of electrons obtained by metal ion (n = 2), N=W/2 = 29. These values are displayed in Fig.3. The average deposition rates, v_1(mg/cm^2·h), determined gravimetrically are also shown in Fig.3 and are compared with those derived theoretically from the I-E curves for partial reactions. It can be seen from Fig.3 that both instantaneous and average deposition rates have similar tendency, i.e., increases with an increasing of the ratio of [NaCit]/[NaCit+NHCit]. This indicates that the species and concentration of ligands have significant influence on the deposition rate.

It is widely accepted that electroless deposition proceeds along the electrochemical mechanism as a simultaneous reaction of cathodic metal deposition and anodic oxidation of a reductant at the same catalytic surface. The difference between the redox potential of the reducing agent and that of the metal, ΔE , is related to the reaction rate. Typically, when ΔE is too large, one can get fast formation of highly dispersed reduction products. To inhibit the reaction, electroless plating baths contain ligands that form strong complexes with metal ions, so it is the complexes instead of free metal ions to be precursors. In the electroless bath with hypophosphite as the reductant, the anodic reaction is the oxidation of hypophosphite:

$$H_2PO_2^- + H_2O = H_2PO_3^- + 2H^+ + 2e$$

The equilibrium potential of the above reaction can be expressed by

$$E_{eq} = -0.504 + \frac{2.3RT}{F}pH + \frac{2.3RT}{2F}\log[\frac{H_2PO_3^-}{H_2PO_2^-}] \qquad (2)$$

where R is the gas constant, T is the temperature, and F is Faraday constant. And cathodic reaction is the reduction of complexing metal ions:

$$ML_m^{2+} + 2e = M + mL$$

$$E_{eq} = E^0_{ML_m/M} + \frac{2.3RT}{2F}\log\beta_m + \frac{2.3RT}{2F}\log[ML^{2+}] \qquad (3)$$

where $E^0_{ML_m/M}$ is the standard redox potential, and β_m is stability constant of metal with complex. The redox potential of the complex depends on the stability constant and the concentration of complexing agent. According to Eq. (3), the increasing of stability constant and/or concentration of complexing agent shifts the potential of deposited metal to the more negative values. In the bath with only sodium citrate as ligand, the metal ions form complexes with citrate, i.e., citrate-iron and citrate-nickel are the precursors. While in the bath with ammonium citrate or these two ligands, the metal ions may form complexes with ammonium and citrate, the citrate-metal, ammonia-metal, and/or citrate-ammonia-metal will serve as precursors [5], the complexing of metal ions causes ΔE to decrease due to the shift of the redox potential of metal ion-metal pair to a more negative region[19-20], thus, the deposition rate decreases with an increasing of NHCit in the bath.

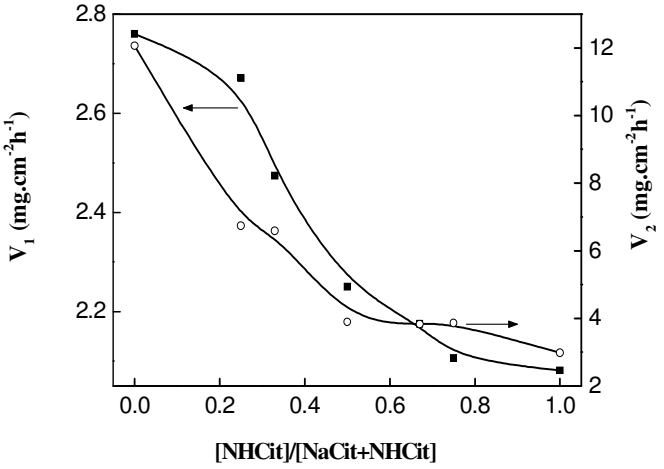

Figure 3. Effect of the ratio of [NHCit]/[NaCit+NHCit] on the deposition rate of Ni- Fe-P films. v_1 and v_2 represent the average deposition rates determined gravimetrically, and the instantaneous deposition rate by polarization measurement, respectively.

Fig.3 also shows that the magnitude of the deposition rate calculated from electrochemical measurement is obviously higher than the average deposition rate by gravimetrical measurement. This is similar with Co-P and Fe-P deposition, which can happen when the cathodic and anodic processes that occur simultaneously are interdependent[17, 21-22]. Another possible explanation is that the autocatalytic process of the Ni-Fe-P reduction is suppressed due to the formation of the iron or nickel hydroxid (phosphides), hydrogen evolution and/or poisoning of the catalytic surface with byproducts of hypophosphite oxidation.

3.3. Effects of ligands on the composition and structure of the thin film

The compositions of the electroless Ni-Fe-P thin films determined by EDS are shown in Table 3. The thin films consist of Ni about 69 atom %, P in the range of 22.80-26.20 atom %, and Fe in the range of 4.83-8.24 atom %. With the increase of the ratio of [NHCit]/[NaCit+NHCit] in bath, nickel content in the thin film changes little, phosphorus content increases, while iron content decreases.

Table 3. Chemical compositions of electroless Ni-Fe-P films

[NHCit]/[NaCit+NHCit]		0	0.5	1
Component Content (atom %)	P	22.80	24.29	26.20
	Fe	8.24	5.91	4.83
	Ni	68.96	69.80	68.97

The XRD patterns of Ni-Fe-P thin films are displayed in Fig.4. All the thin films show typical amorphous diffraction patterns with broad peaks. It is obvious that, with the increase of the ratio of [NHCit]/[NaCit+NHCit], the full widthes at half maximum of these peaks increase. The peak broadening suggests a greater tendency to form amorphous structure, which is largely due to the increase of phosphorus content in the thin film. This is consistent with others results[5,23].

Electroless deposition process is an autocatalytic process with the metal as a final product due to the chemical reduction of the metal cations through reductants in the bath. In the electroless bath with hypophosphite as the reductant, the anodic reaction is the oxidation of hypophosphite:

$$H_2PO_2^- + H_2O \rightarrow H_2PO_3^- + 2H^+ + 2e$$

And at the same time, the electrons released by the oxidation reaction of hypophosphite take part in the cathodic reactions, i.e., were used to reduction Fe^{2+}, Ni^{2+}, H^+ and/or $H_2PO_2^-$ competively. The cathodic reactions can be presented as follows

$$Ni^{2+} + 2e \rightarrow Ni$$
$$2H^+ + 2e \rightarrow H_2$$
$$H_2PO_2^- + 2H^+ + e \rightarrow P + H_2O$$
$$Fe^{2+} + 2e \rightarrow Fe$$

In the bath with NHCit as ligands, the polarization resistance increased and the reducing ability of Fe^{2+}, Ni^{2+} ions decreased due to the formation of $[Ni(NH_3)_n]^{2+}$, $[Fe(NH_3)_n]^{2+}$, more electrons are captured by $H_2PO_2^-$ and the phosphorus content in the thin films increased. Thus the change of

composition and structure of the thin film may be attributed to the competitive reduction of several ions, such as nickel ions, hydrogen ions, iron ions, and hypophosphite anion. The work is beneficial for the structure adjustment and performance improvement of electroless thin films by optimization the bath component.

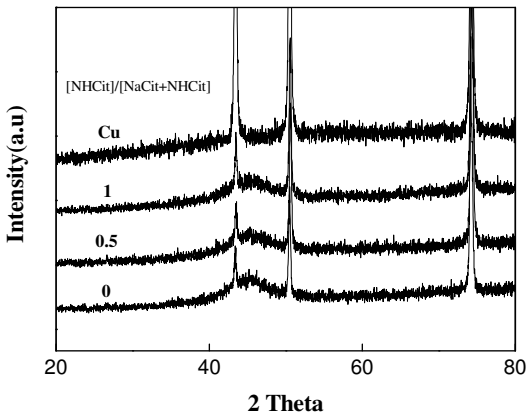

Figure 4. The XRD patterns of Ni-Fe-P thin film deposited from the bath with different [NHCit]/[NaCit+NHCit] ratio

4. CONCLUSIONS

Ligand effects the deposition process, deposition rate, composition, and structure of the electroless Ni-Fe-P thin films. With the increasing of [NHCit]/[NaCit+NHCit], the resistance for redox reactions increases, the electroless deposition systems are more polarized, the oxidation of $H_2PO_2^-$ and the formation of Ni-Fe-P thin films are inhibited, thus mixed potential shifts positively and deposition rate decreases. The magnitude of the deposition rate calculated from electrochemical measurement is higher than the average deposition rate determined by gravimetrical measurement due to interdependency between cathodic and anodic processes and the by-reaction such as the formation of metal hydroxid and hydrogen evolution. All the thin films display typical amorphous nature. As the ratio of [NHCit]/[NaCit+NHCit] increases, nickel content in the thin film changes little, phosphorus content increases, while iron content decreases, leading to the increase of amorphous degree of thin films.

ACKNOWLEDGEMENTS
This work was supported by Hunan Provincial Natural Science Foundation of China (Grant No. 05JJ30089).

References

1. I.Baskaran, T.S.N. Sankara Narayanan, A.Stephen, *Mater.Chem.Phys*. 99(2006) 117
2. A.Vaskelis, J. Jaciauskiene, I.Stalnioniene, E.Norkus, *J.Electroanal.Chem*. 600(2007)6
3. Y.M. Lin, S.C. Yen, *Appl. Surf. Sci.* 178 (2001)116
4. F. Hanna, Z.A. Hamid, A.A. Aal, *Mater. Lett*. 58 (2004)104
5. X.C. Wang, W.B. Cai, W.J. Wang, et al., *Surf. Coat. Tech*. 168 (2003)300
6. M.E. Touhami, M. Cherkaoui, A. Srhiri, A. Ben Bachir, *J.Appl. Electrochem*. 26 (1996)487
7. E. Norkus, A. Vaskelis, I. Stalnioniene, *J. Solid State Electrochem*. 4(2000)337
8. M. Paunovic, *J. Electrochem. Soc.* 124 (1977)349
9. A.F. Schmeckenbecher, *J. Electrochem. Soc*. 113(1966)778
10. H. Matsubara, T. Yonekawa, Y. Ishino, et al., *Electrochim. Acta* 52 (2006)402
11. L.L. Wang, L.H. Zhao, G.F. Huang, *Surf. Coat. Tech*. 126(2000)272
12. T. Osaka, *Electrochim. Acta* 44 (1999)3885
13. G. Gabrielly, F. Raulin, *J. Appl. Electrochem.* 1 (1971)167
14. J. Kivel, J.S. Sallo*, J. Electrochem. Soc*. 112 (1965)1201
15. J.N. Balaraju, V. Ezhil Selvi, V.K. William Grips, et al., *Electrochim. Acta* 52 (2006)1064
16. S.L. Wang, *Surf. Coat. Tech*. 186 (2004)372
17. G.F. Huang, J.-Q. Deng,W.Q. Huang, et al., *Int. J. Electrochem. Sci.* 2 (2007)72
18. N. Eliaz, E. Gileadi, *ECS Transactions*, 2 (2007) 337
19. N.Petrov, Y.Sverdlov, Y. Shacham-Diamand, *J. Electrochem. Soc*. 149(2002)C187
20. M. Supicova, R. Orinakova, M. Kupkova, et al., *Surf. Coat. Tech*. 195 (2005)130
21. I.Ohno, S. Haruyama, *Surf.Technol*., 13(1981)1
22. G.F. Huang, W.Q. Huang, L.L. Wang, et al., *Electrochim. Acta* 51(2006) 4471
23. H. Ashassi-Sorkhabi, S. H. Rafizadeh, *Surf. Coat. Tech*. 176 (2004)318